Periodically forced food-chain dynamics: model predictions and experimental validation

Christopher F. Steiner,[1,2,6] Anne S. Schwaderer,[2,3] Veronika Huber,[4] Christopher A. Klausmeier,[2,5] and Elena Litchman[2,3]

[1]*Department of Biological Sciences, Wayne State University, Detroit, Michigan 48202 USA*
[2]*W. K. Kellogg Biological Station, Michigan State University, Hickory Corners, Michigan 49060 USA*
[3]*Department of Zoology, Michigan State University, East Lansing, Michigan 48824 USA*
[4]*Potsdam Institute for Climate Impact Research, Telegrafenberg A31, 14473 Potsdam, Germany*
[5]*Department of Plant Biology, Michigan State University, East Lansing, Michigan 48824 USA*

Abstract. Despite the recognition of the importance of seasonal forcing in nature, remarkably few studies have theoretically explored periodically forced community dynamics. Here we employ a novel approach called "successional state dynamics" (SSD) to model a seasonally forced predator–prey system. We first generated analytical predictions of the effects of altered seasonality on species persistence and the timing of community state transitions. We then parameterized the model using a zooplankton–phytoplankton system and tested quantitative predictions using controlled experiments. In the majority of cases, timing of zooplankton and algal population peaks matched model predictions. Decreases in growing-period length delayed algal blooms, consequently delaying peaks in zooplankton abundance. Predictions of increased probability of predator extinction at low growing-period lengths were also upheld experimentally. Our results highlight the utility of the SSD modeling approach as a framework for predicting the effects of altered seasonality on the structure and dynamics of multitrophic communities.

Key words: Brachionus calyciflorus; Chlamydomonas reinhardtii; environmental forcing; periodic mortality; phytoplankton; predator–prey dynamics; seasonal succession; seasonality; transient dynamics; zooplankton.

Introduction

Approaches to modeling consumer–resource interactions have frequently relied on the assumption that systems are at equilibrium and that parameters governing species vital rates are fixed through time. While such approaches have proven powerful in identifying key ecological mechanisms and processes, most ecologists recognize that many natural systems experience temporally varying environmental conditions that can buffet populations, enhance background mortality rates, and drive population trajectories far from steady-state conditions. Hence, perceived patterns of community structure may actually be in flux as populations are frequently within transitory phases due to external forcing (Hastings 2001, 2004, Jäger et al. 2008). The overriding influence of temporal heterogeneity on community dynamics is most readily apparent in temperate and high-latitude systems in which seasonal variation imposes periods of active somatic and population growth followed by periods of depressed metabolic activity, dormancy, and increased mortality. Predicting the long-term consequences of such periodic

forcing on the dynamics and structure of communities is a challenge to ecologists and may prove especially vital in the near future as large-scale climate change threatens to alter the strength and timing of seasonality in many natural systems (Walther et al. 2002, Parmesan and Yohe 2003).

Despite the recognition of the importance of temporal variability and seasonal forcing in nature, remarkably few studies have theoretically explored how periodic mortality events alter community dynamics within spatially homogeneous, closed systems (but see Scheffer et al. 1997, Ives et al. 2000). One obstacle to theoretical advancement is the lack of analytical techniques for exploring the effects of large perturbations with long period lengths. Recently, C. A. Klausmeier (*unpublished manuscript*) outlined a general methodology for theoretically examining the effects of seasonal mortality events on community dynamics, based on earlier work (Litchman and Klausmeier 2001). Called "successional state dynamics" (SSD), the model framework treats compositional succession of a community as a path taken through different community equilibria during an active growing period that is periodically reset to a near-empty state during a period of intensified mortality (e.g., the winter season).

Here we employ the SSD approach to model the dynamics of a periodically forced food chain composed
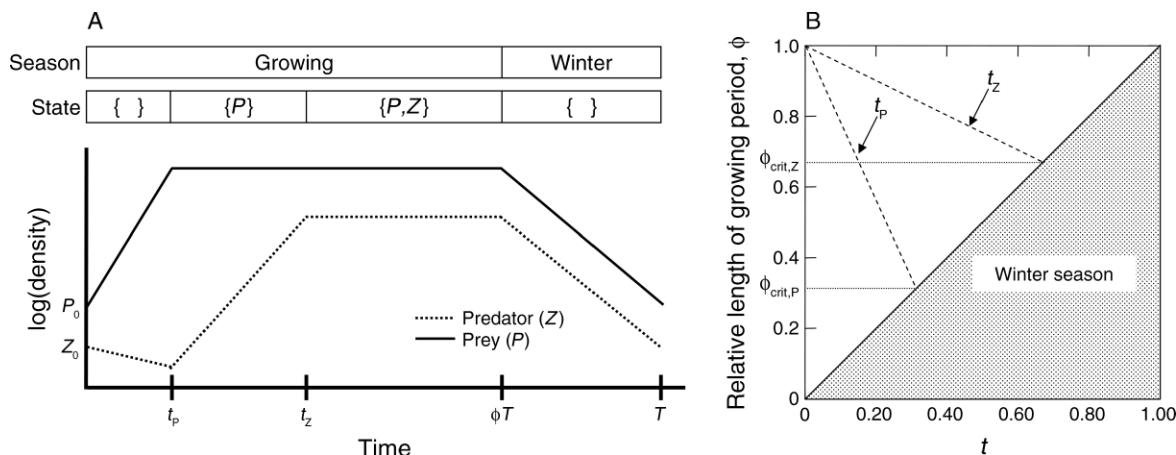
FIG. 1. General predictions of the successional state dynamics (SSD) food-chain model in which length of the year (T) has been standardized to equal 1 (shown are predictions for a hypothetical predator and prey). (A) An example of predator and prey dynamics over a single growing season in which relative growing-period length (ϕ) is long enough to permit both predator and prey persistence. At the start of the growing season the community transitions from the empty state { }, to the prey-only state $\{P\}$ at time t_P, to the predator-and-prey state $\{P, Z\}$ at time t_Z, and back to the empty state at time ϕT. (B) Predicted transition times (dashed diagonal lines) to the prey-only state (t_P) and the prey and predator present state (t_Z) for a range of ϕ values. As the length of the growing season increases toward a limit of $\phi = 1$ (no winter season), the predicted timings converge toward $t = 0$ and a state in which both predator and prey persist at equilibrium densities for the duration of the year. Decreasing the proportion of the year devoted to growth relative to the winter (decreasing ϕ) causes prey to invade later in the growing period and delays the state transition from prey alone to predator plus prey. Shown also are critical ϕ values that permit invasion and persistence by the prey ($\phi_{crit,P}$) and the predator ($\phi_{crit,Z}$).

of a single top predator and a single prey. We generate quantitative predictions of the effects of growing-season length on the timing of key state transitions of the system using a simple planktonic system as a model basis. We then test these predictions using controlled laboratory experiments. Planktonic communities are excellent model systems for examining the impacts of seasonal forcing on community dynamics as they are known to exhibit repeatable patterns of seasonal succession in nature (Sommer et al. 1986, Sommer 1989). Moreover, alterations in seasonality and growing-season length are believed to have strong effects on zooplankton–algal dynamics and the timing of key events such as spring algal blooms, peaks in zooplankton abundance, and the clear-water phase (Straile and Adrian 2000, Straile 2002, Mooij et al. 2005, Berger et al. 2007, Huber et al. 2008). Hence, model development and experimental validation using the simplified modules of these systems are important first steps toward understanding natural variation in seasonal patterns.

Model predictions

In-depth analysis of the effects of periodic forcing on community dynamics using the SSD approach will be presented in a future paper (C. A. Klausmeier, *unpublished manuscript*). Here we outline the salient features and predictions of the SSD food-chain model. The SSD approach models seasonal succession as a path through possible community equilibria (or "states") of the non-forced system. In a system composed of a single zooplankton predator (Z) and its phytoplankton prey

(P), there are three possible community states: prey present and predator absent, predator and prey both present, and the empty state (both predator and prey absent). Given these possible states, there are only two nontrivial successional trajectories the system may take following winter mortality: (1) the empty state to prey present and (2) the empty state to prey present to a state with both predator and prey present. The SSD model assumes that changes in log-transformed predator and prey densities approach a linear form over time (Fig. 1A). Note that in Fig. 1 and henceforth the length of the year (T) has been standardized to equal 1. In a system that can support zooplankton and phytoplankton, phytoplankton invade the empty state { } at initial density (P_0) following winter and increase exponentially at their maximal growth rate until reaching a threshold density (K_P) at time t_P (Fig. 1A). Zooplankton enter the empty state { } at initial density (Z_0) and decline at their background mortality rate during this phase. In the prey-only state $\{P\}$, phytoplankton are at a threshold level and zooplankton increase at their maximal growth rate until peaking at their threshold density (K_Z) at time t_Z. In this state $\{P, Z\}$, both zooplankton and phytoplankton populations are unchanging until the final empty state { }, when both populations experience winter mortality. As population dynamics in these different phases are simple functions of exponential growth and mortality rates, they can be easily represented mathematically. The long-term population growth rate of phytoplankton (Λ_P) averaged over a period is as follows:

$$\Lambda_{\mathrm{P}} = \lambda_{\mathrm{P},\{\},\mathrm{G}} t_{\mathrm{P}} + \lambda_{\mathrm{P},\{\},\mathrm{W}}(1-\phi) \qquad (1)$$

where $\lambda_{\mathrm{P},\{\},\mathrm{G}}$ is its growth rate when invading the empty state early in the growing season, t_{P} is the proportion of the year required for phytoplankton to reach equilibrium when invading (after which net growth rate equals 0), and $\lambda_{\mathrm{P},\{\},\mathrm{W}}$ is its mortality rate during the winter season weighted by the proportion of the year that is winter $(1-\phi)$. For the invading predator (Z), long-term growth averaged over a period is

$$\Lambda_{\mathrm{Z}} = \lambda_{\mathrm{Z},\{\},\mathrm{G}} t_{\mathrm{P}} + \lambda_{\mathrm{Z},\{\mathrm{P}\},\mathrm{G}}(t_{\mathrm{Z}} - t_{\mathrm{P}}) + \lambda_{\mathrm{Z},\{\},\mathrm{W}}(1-\phi) \quad (2)$$

where $\lambda_{\mathrm{Z},\{\},\mathrm{W}}$ is the predator's winter mortality rate, $\lambda_{\mathrm{Z},\{\},\mathrm{G}}$ is its growth rate when invading the empty state (which is assumed to be negative and equal to its background mortality), and $\lambda_{\mathrm{Z},\{\mathrm{P}\},\mathrm{G}}$ is its exponential growth rate following successful prey invasion (at time t_{P}) which proceeds until the predator reaches an equilibrium density at time t_{Z}.

Model predictions of the effects of relative length of the growing period (ϕ) on the timing of state transitions can be easily ascertained by assuming that the system has settled to a stable seasonal trajectory, setting Eqs. 1 and 2 to 0 and solving for t_{P} and t_{Z} (C. A. Klausmeier, *unpublished manuscript*). Doing so produces the following relationships:

$$t_{\mathrm{P}} = \frac{-\lambda_{\mathrm{P},\{\},\mathrm{W}}(1-\phi)}{\lambda_{\mathrm{P},\{\},\mathrm{G}}} \qquad (3)$$

$$t_{\mathrm{Z}} = \frac{-\lambda_{\mathrm{Z},\{\},\mathrm{G}} t_{\mathrm{P}} + \lambda_{\mathrm{Z},\{\mathrm{P}\},\mathrm{G}} t_{\mathrm{P}} - \lambda_{\mathrm{Z},\{\},\mathrm{W}}(1-\phi)}{\lambda_{\mathrm{Z},\{\mathrm{P}\},\mathrm{G}}}. \qquad (4)$$

Furthermore, critical ϕ values that permit successful invasion of predator and prey can also be determined. The minimum ϕ permitting invasion and persistence by the prey $(\phi_{\mathrm{crit,P}})$ is found by setting $\phi_{\mathrm{crit,P}} = \phi = t_{\mathrm{P}}$ and solving Eq. 3. Similarly, the minimum ϕ permitting predator invasion $(\phi_{\mathrm{crit,Z}})$ is found by setting $\phi_{\mathrm{crit,Z}} = \phi = t_{\mathrm{Z}}$ in Eq. 4 and solving for $\phi_{\mathrm{crit,Z}}$. Doing so produces the following:

$$\phi_{\mathrm{crit,P}} = \frac{\lambda_{\mathrm{P},\{\},\mathrm{W}}}{\lambda_{\mathrm{P},\{\},\mathrm{W}} - \lambda_{\mathrm{P},\{\},\mathrm{G}}} \qquad (5)$$

$$\phi_{\mathrm{crit,Z}} = \big(\lambda_{\mathrm{Z},\{\},\mathrm{W}}\lambda_{\mathrm{P},\{\},\mathrm{G}} + \lambda_{\mathrm{Z},\{\mathrm{P}\},\mathrm{G}}\lambda_{\mathrm{P},\{\},\mathrm{W}}$$

$$- \lambda_{\mathrm{Z},\{\},\mathrm{G}}\lambda_{\mathrm{P},\{\},\mathrm{W}}\big)$$

$$\div \big(\lambda_{\mathrm{Z},\{\},\mathrm{W}}\lambda_{\mathrm{P},\{\},\mathrm{G}} - \lambda_{\mathrm{Z},\{\},\mathrm{G}}\lambda_{\mathrm{P},\{\},\mathrm{W}}$$

$$- \lambda_{\mathrm{Z},\{\mathrm{P}\},\mathrm{G}}\lambda_{\mathrm{P},\{\},\mathrm{G}} + \lambda_{\mathrm{Z},\{\mathrm{P}\},\mathrm{G}}\lambda_{\mathrm{P},\{\},\mathrm{W}}\big). \qquad (6)$$

General predictions from Eqs. 3–6 are fairly intuitive and shown in Fig. 1B. Dashed lines represent predicted timings of state transitions (t) in relation to relative growing-period length (ϕ). Shown are predictions for transitions to the prey-only state $\{P\}$ and the prey-and-

predator present state $\{P, Z\}$. As the length of the growing season increases toward a limit of $\phi = 1$ (no winter season), the predicted timings converge toward $t = 0$ and a state in which both predator and prey persist at equilibrium densities for the duration of the year. Decreasing the proportion of the year devoted to growth relative to the winter (decreasing ϕ) increases the severity of winter mortality. Consequently, prey invade the system later in the growing period and the state transition from prey alone to predator plus prey is delayed (Fig. 1B). If the growing season is too short (below $\phi_{\mathrm{crit,Z}}$ in Fig. 1B), predators are unable to invade and persist and the system only transitions to a state with the prey present; growing seasons less than $\phi_{\mathrm{crit,P}}$ exclude both predators and prey.

We tested the SSD model predictions using an experimental food chain composed of a single species of zooplankton as a predator and a single species of phytoplankton as its prey. We empirically derived estimates of exponential growth and background mortality rates for our species and then generated quantitative predictions of critical ϕ values ($\phi_{\mathrm{crit,P}}$ and $\phi_{\mathrm{crit,Z}}$) and the timing of state transitions (t_{P} and t_{Z}) under different growing-period lengths. These predictions were then compared to observed experimental transition times and patterns of zooplankton/phytoplankton persistence.

METHODS

Experimental system

Experiments were conducted using a laboratory-based system consisting of the rotifer *Brachionus calyciflorus* as a predator and the flagellated green alga *Chlamydomonas reinhardtii* as its prey (all species are hereafter referred to by genus). We obtained *Brachionus* cultures from Florida Aqua Farms (Dade City, Florida, USA), while *Chlamydomonas* was a wild-type strain (number CC-2935) obtained from the *Chlamydomonas* Genetics Center (Duke University, Durham, North Carolina, USA). *Brachionus* cultures were fed the same *Chlamydomonas* strain used in the experiment and all stock cultures were maintained using the same medium and environmental conditions as in the experiment. Experimental vessels consisted of 1000-mL flasks loosely capped with aluminum foil and filled with 800 mL of COMBO medium; medium was prepared as in Kilham et al. (1998) except that phosphorus was added at a lowered concentration of 490 μg/L to minimize formation of nonmotile algal cells (Harris 1989). All flasks were housed and randomly ordered in a single environmental chamber at 25°C under 24-hour light; flasks were rotated on the chamber shelves daily. During the experiment, flasks were manually mixed and had 10% of their volume removed and replaced with fresh medium once daily (removed medium served as a zooplankton and phytoplankton sample). Both *Brachionus* and *Chlamydomonas* are motile and found in the water column; manual mixing helped ensure that nutrients and organisms

remained relatively homogeneous in their distributions. *Brachionus* were enumerated using a dissecting scope while *Chlamydomonas* were counted using a CASY particle counter (Scharfe System, Reutlingen, Germany). As *Brachionus* males do not actively feed and were rare, population densities of *Brachionus* were based only on counts of females. All experimental materials were autoclave-sterilized prior to use.

We tested the capacity of our model to predict the timing of state transitions for different relative growing-period lengths. Experimentally, the proportion of the year devoted to the growing period (ϕ) vs. winter can be easily manipulated by periodically imposing different levels of winter mortality via a single, large-scale mortality event. For example, an imposed mortality event of 90% of the community would correspond to a longer winter period compared to a mortality event with 50% removal. We employed five relative growing-period treatments: $\phi = 0.65$, 0.70, 0.75, 0.80, and 0.85, with each treatment replicated 4 times. Our previous pilot experiments and model simulations showed that *Brachionus* and *Chlamydomonas* could persist at these ϕ levels and that the $\phi = 0.65$ treatment was close to the critical ϕ ($\phi_{crit,Z}$) for *Brachionus*, allowing us to test the effects of decreased ϕ on the probability of predator extinction. To experimentally impose winter mortality, a percentage of the community was removed by volume from each flask, added to a new flask and then brought to 800 mL total with fresh, sterile medium. Percentage of volume, D, removed for each treatment was calculated using $D = \exp(\lambda_{\{\},W}(1 - \phi)T')100$, where $\lambda_{\{\},W}$ is the winter mortality rate for both predator and prey arbitrarily set to $-1/d$, and T' is the absolute length of the full period (growing season plus winter). T' can be easily calculated from $\phi T' = t_{max}$ where t_{max} is the time the organisms where allowed to grow between mortality events (set to 14 days for all treatments). A 14-day growing length was chosen based on preliminary experiments that showed that *Brachionus* densities peaked and equilibrated by day 14.

At the start of the experiment, 20 cells/mL of *Chlamydomonas* were added to all experimental flasks. Algae were allowed to reproduce for seven days at which time *Brachionus* individuals were haphazardly isolated from stock cultures and added at a density of 0.125 individuals/mL. Zooplankton were allowed to reproduce for 14 days, reaching a peak in density; we refer to this initial growth period as "year 0." On day 14, the first winter-mortality event was imposed and communities were allowed to numerically respond for 14 days; we refer to this growth period as "year 1." A second winter mortality was then imposed and communities were again allowed to respond for another 14 days ("year 2") at which time the experiment was terminated.

Quantitative predictions and data analysis

To generate quantitative predictions of the timing of state transitions for our treatments, we parameterized our model using data from year 1 of the experiment. Estimates of species growth rates, background mortality rates (λ's), initial densities (phytoplankton, P_0, and zooplankton, Z_0) and threshold densities (K_p and K_z) were obtained by fitting the log-linear SSD (successional state dynamics) model structure (as in Fig. 1A) simultaneously to ln-transformed *Brachionus* and *Chlamydomonas* densities using a genetic algorithm (Haupt and Haupt 1998). Unlike conventional parametric model fitting, we employed a rule-based approach to obtain the SSD model fits. Fitting the SSD model structure translates to parameterizing rules that are used to numerically project the community forward in time as in Fig. 1A (C. A. Klausmeier, *unpublished manuscript*). These rules dictate λ's based on the state of the system and determine how state transitions occur in the system. Specifically, populations grow or shrink exponentially at rates determined by the current state of the system (i.e., which species are at their threshold abundances). Transitions take place when a population is projected to reach its threshold abundance or when winter occurs. The procedure consisted of repeating the following steps: (1) time increments to all potential state transitions are calculated; (2) the temporally closest transition is chosen to occur; and (3) population densities and the state of the system are updated accordingly (C. A. Klausmeier, *unpublished manuscript*). While conventional gradient-search methods are not appropriate for this type of rule-based model parameterization, other optimization techniques such as genetic algorithms can easily handle these problems. For details on the genetic algorithm procedure used see Appendix B. Models were fit to data from each treatment replicate separately. After obtaining λ estimates for each replicate from the model fits, critical ϕ values ($\phi_{crit,P}$ and $\phi_{crit,Z}$) were calculated by solving Eqs. 5 and 6 for all possible combinations of λ's ($n = 20$ for $\phi_{crit,P}$, and $n = 20^3$ for $\phi_{crit,Z}$). Similarly, we calculated transition times (t_P and t_Z) based on all combinations of λ's (Eqs. 3 and 4) for all treatment-level ϕ values ($\phi = 0.65$, 0.7, 0.75, 0.8, and 0.85). Predictions for mean critical ϕ values and transition times were determined by calculating the mean (and standard deviations) of the resultant distributions.

Model predictions generated from our year-1 model fits were compared to observed transition times from year 2 of the experiment. To estimate transition times in year 2, we again fit the SSD log-linear model to ln-transformed year-2 data for each replicate separately using the genetic algorithm (as for year 1). This yielded estimates for initial densities (P_0 and Z_0), threshold densities (K_P and K_Z) and vital rates (λ's) for each replicate. Instead of calculating transition times using Eqs. 3 and 4 (as for year 1), these parameters were used to numerically determine transition times. We employed the same method described above to numerically project the community forward in time; transitions were determined to take place when a population was
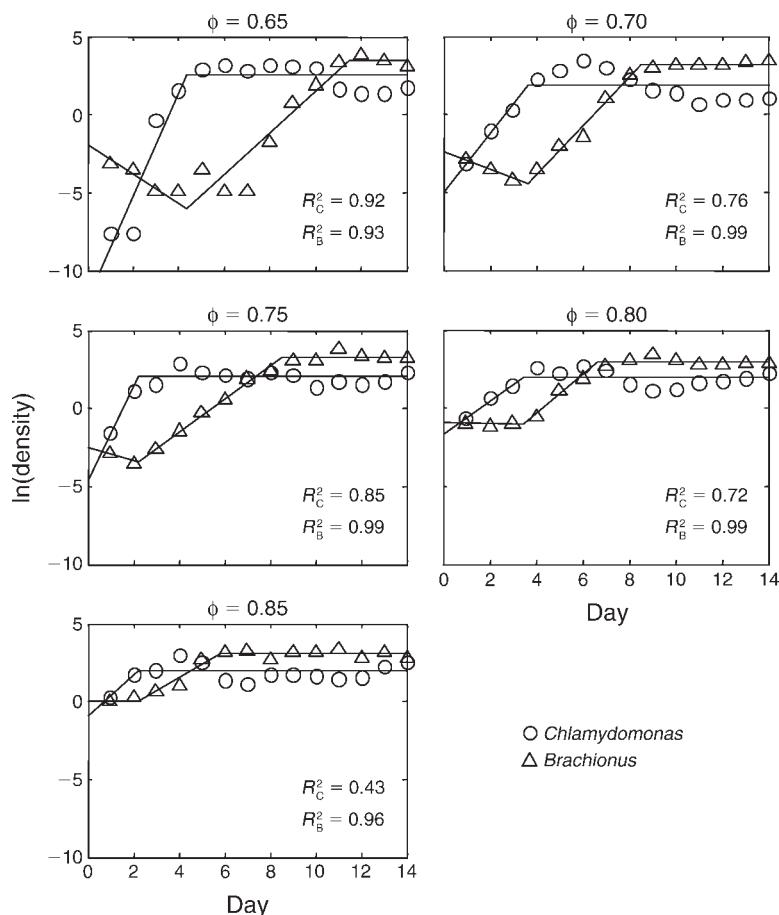
FIG. 2. Dynamics of the zooplankton predator *Brachionus* and the algal prey *Chlamydomonas* in year 2 of the experiment following winter mortality. Shown are example replicates for each relative growing-period treatment (ϕ). The R^2 subscripts refer to genus names. *Brachionus* densities were measured as number of individuals/mL; *Chlamydomonas* densities were rescaled to individuals/10^{-5} mL. Results are for replicate number 2 (year 1 and year 2 data and fits for all replicates can be found in Appendix A).

projected to reach its threshold abundance or when winter occurred (C. A. Klausmeier, *unpublished manuscript*). All transition times are presented as proportions of the full period (winter plus growing seasons). Observed and mean predicted transition times were compared using one-sample *t* tests. We also calculated type II error rates (β values) for each *t* test and its observed *P* value. In a few rare instances, *Brachionus* and *Chlamydomonas* densities fell below the limits of sampling detection following winter mortality. Rather than exclude these data points, we added a constant to these values equivalent to the detection-limit density. Model fitting was performed using MATLAB (MATLAB 2006); statistical tests were performed using SYSTAT (SPSS 2000).

RESULTS

Time series and model fits for all treatments and replicates can be found in the supplementary figures (Appendix A: Figs. A1 and A2). Model fits converged quickly for both years 1 and 2 with parameter estimates

exhibiting negligible change over time and high congruence among repeated reinitializations of the genetic algorithm after 300 000 generations (Appendix A: Fig. A3). In general, the log-linear SSD model captured observed *Brachionus* dynamics well, with the majority of R^2 values greater than 0.90 (Fig. 2; Appendix A: Figs. A1 and A2). Model fits were weaker for *Chlamydomonas*, accounting for a smaller proportion of variation compared to *Brachionus* in all replicates (Fig. 2; Appendix A: Figs. A1 and A2). Lower R^2 values for *Chlamydomonas* were largely due to declines in algal abundance following invasion by *Brachionus*.

Transition times observed in year 2 of our experiment and model predictions for each treatment level are listed in Table 1. Fig. 3 displays means from the model prediction distributions and mean observed transition times. As can be seen, observed transition times in year 2 showed good qualitative agreement with model predictions (Fig. 3; Table 1). As the relative length of the growing period was reduced, both t_P and t_Z were predicted to occur later in the growing season. This

TABLE 1. Mean predicted and mean observed transition times for phytoplankton (t_P) and zooplankton (t_Z) for each relative growing-period treatment (ϕ).

					Observed vs. predicted			
Relative length of growing period, ϕ	Mean predicted		Mean observed		t_P		t_Z	
	t_P	t_Z	t_P	t_Z	P	β	P	β
0.65	0.216	0.491	0.202	0.500	0.034	0.000	0.817	0.176
0.7	0.185	0.456	0.180	0.442	0.478	0.406	0.453	0.415
0.75	0.154	0.416	0.162	0.384	0.718	0.262	0.320	0.446
0.8	0.123	0.368	0.144	0.393	0.415	0.427	0.058	0.425
0.85	0.093	0.283	0.162	0.382	0.052	0.423	0.037	0.418

Note: P values and type II error rates (β) are for one-sample t tests comparing observed and predicted transition times.

trend was observed for both *Brachionus* and *Chlamydomonas* but was only strongly expressed at lower ϕ values, i.e., at higher levels of seasonal forcing (Fig. 3). Delays in *Chlamydomonas* transition times were evident at the four lowest ϕ treatments while *Brachionus* exhibited delays at the three lowest ϕ treatments (Fig. 3).

Quantitative agreement with model predictions was strongest for *Chlamydomonas* at ϕ levels 0.7–0.8 (Table 1). Differences between observed and predicted transition times for these treatments were weak, exhibiting P values all greater than 0.40 (Table 1), while differences were evident in the $\phi = 0.65$ and $\phi = 0.85$ treatments (Table 1). Type II error rates for ϕ levels 0.7–0.8 also were moderate to high, ranging between 0.26 and 0.43 (Table 1). Thus, there was a reasonably high probability of failing to detect differences between our observed and predicted transition times when differences may have actually been present in these treatments. Quantitative agreement between observed and predicted transition times for *Brachionus* were strongest in the three lowest ϕ treatments (Table 1); significant differences were only detected at the two highest ϕ levels (Table 1). As with *Chlamydomonas*, type II error rates were also fairly high for several of the treatments in which no significant differences were detected (Table 1).

Year-1 fits produced mean critical ϕ values of $\phi_{crit,P} = 0.37$ (SD = 0.11) for *Chlamydomonas* and $\phi_{crit,Z} = 0.63$ (SD = 0.09) for *Brachionus* (Fig. 3). The latter value was close to our lowest ϕ treatment ($\phi = 0.65$; Fig. 3), and *Brachionus* indeed went extinct in two replicates of this treatment following winter mortality in year 2 (extinction was verified by exhaustively sampling flasks at the termination of the experiment). These replicates were excluded from analyses.

DISCUSSION

While most ecologists recognize the potential of periodic forcing to strongly impact community dynamics, theoretical examinations have remained surprisingly uncommon. This is particularly true of freshwater planktonic systems in which seasonal succession is a well-recognized facet of temperate systems, receiving profuse empirical investigation, but where theoretical treatments and quantitative modeling of seasonal dynamics have been rare (though see Scheffer et al.

[1997] and de Senerpont Domis et al. [2007]). The SSD (successional state dynamics) approach offers a tractable technique for examining generalizable food-web structures within a dynamic seasonal framework, permitting analytical and quantitative predictions of the effects of altered seasonality on patterns of species coexistence and the timing of community state transitions.

For simple food chains, the SSD model predicts that increasing the length of the growing season relative to winter increases the probability of predator–prey persistence. This prediction was supported by our experimental system. *Brachionus* populations persisted in the four highest of five relative growing-period treatments, ϕ, for the duration of the experiment but went extinct at the start of year 2 in two replicates of the $\phi = 0.65$ treatment, the treatment with the shortest relative growing period and most severe winter mortality. This treatment level was very close to the critical ϕ
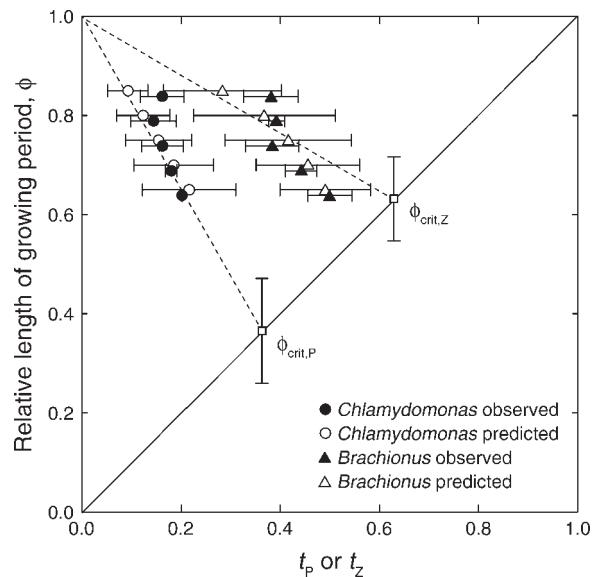

FIG. 3. Predicted and observed transitions times (means ± SD) for *Chlamydomonas* (t_P) and *Brachionus* (t_Z). Observed values have been offset vertically to better display error bars. Shown also are predicted critical ϕ values (mean ± SD) for *Chlamydomonas* ($\phi_{crit,P}$) and *Brachionus* ($\phi_{crit,Z}$) (open squares). The dashed lines are extrapolated predictions from the critical ϕ values (as in Fig. 1B).

for *Brachionus* predicted by our model ($\phi_{\mathrm{crit},Z} = 0.63$) below which extinction is expected.

In addition to facilitating predator/prey persistence, increasing growing-period length relative to winter was predicted to hasten invasion by both predator and prey during the active growing season. Thus, transition times (t_P and t_Z) were expected to occur earlier in the year with increasing levels of ϕ. This prediction is consistent with long-term patterns of zooplankton–algal dynamics in natural systems in which warming trends have advanced seasonal community development (e.g., Straile 2002). Our experiment provided further evidence of shifts in successional dynamics with altered seasonality; both the algal prey *Chlamydomonas* and the zooplankton predator *Brachionus* exhibited accelerated transitions times with increasing ϕ, although effects of extended growing seasons on zooplankton–algal peaks were more strongly expressed in the lower ϕ treatments. For both *Chlamydomonas* and *Brachionus*, observed transition times tended to occur later than predicted at the two highest period lengths ($\phi = 0.80$ and 0.85).

Deviations between observed and predicted timings could be due to several factors. First, a key assumption when generating our model predictions was that the system had settled onto a stable seasonal trajectory. This assumes that species' initial densities at the start of the growing season are unchanging from year to year. However, it was possible that two rounds of winter mortality were insufficient to attain stability in our experimental system. When comparing *Chlamydomonas* initial densities obtained from our model fits for each replicate, we found no differences between years (Appendix A: Fig. A4). However, *Brachionus* showed evidence of lower initial densities in year 2 compared to year 1 with differences being strongest in the three highest ϕ treatments (Appendix A: Fig. A4). Low densities early in the growing period should translate into delayed peaks in abundance later in the growing period potentially explaining t_Z values higher than predicted.

Another assumption of our model was that species' vital rates (λ) were constant across ϕ treatments and across years. This assumption was not upheld in our experimental system. First, the large standard deviations exhibited by our prediction distributions (Fig. 3) expose the large amount of variation in λ estimates among replicates in year 1. This variation was not only generated by process and measurement error but by variation among treatments as well; significant differences in *Brachionus* growth rates were detected among ϕ levels in year 1 (Appendix A: Fig. A5). Furthermore, variation among treatments was also evident in year 2; *Brachionus* growth rates were higher than the year-1 average for the three lowest ϕ treatments and lower than the year-1 average for the two highest ϕ treatments (Fig. 4). A similar trend was observed for *Chlamydomonas* growth rates; however differences among treatments were statistically weaker (Appendix A: Fig. A6).
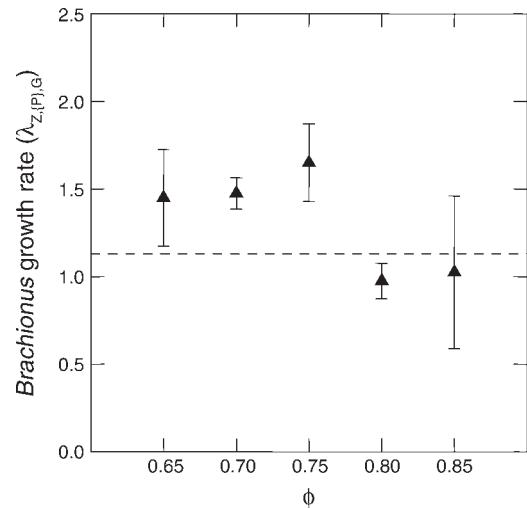

Fig. 4. Variation in *Brachionus* growth rates following prey invasion ($\lambda_{Z,\{P\},G}$) across ϕ treatments in year 2. Data are means $\pm$ SE. The dashed line represents the mean growth rate generated from year 1 (averaged across ϕ treatments). There was a weak effect of ϕ on $\lambda_{Z,\{P\},G}$ using one-way ANOVA ($P = 0.09$).

Systematic variation in *Brachionus* invasion rates with growing-period length may account for deviations between observed and predicted t_Z values. Lower than average rates in the $\phi = 0.80$ and 0.85 treatments should lead to transition times that occur later than mean predicted timings.

We can only speculate on the cause of variation in zooplankton growth rates among our treatments. One possibility is that algal nutritional quality varied among ϕ treatments early in the growing period. In treatments with shorter growing periods, *Chlamydomonas* populations started at much lower densities at the initiation of the growing season and thus experienced exponential growth for longer periods of time. For example, algal densities, on average, increased up to four orders of magnitude in the $\phi = 0.65$ treatment and less than two orders of magnitude in the $\phi = 0.85$ treatment in year 2 (Fig. 2). Algal populations that experience nutrient-saturated conditions and exponential growth for longer periods of time should exhibit higher cellular nutrient content (i.e., lower carbon:phosphorus and carbon:nitrogen content) and thus could be of greater nutritional quality for zooplankton. Moreover, *Chlamydomonas* cells grown under nutrient-saturated conditions are known to be more easily digested by zooplankton compared to nutrient-limited cells (Van Donk et al. 1997), further increasing the probability that algal populations in low ϕ treatments were of better quality for *Brachionus*. Whether covariation between zooplankton maximal growth rates and growing-season length is a peculiarity of our model system or a generalizable feature of natural planktonic systems is an open question. While our highly simplified system may have amplified such effects, it is not inconceivable that this

phenomenon could occur in natural systems, delaying expected zooplankton population peaks. If of sufficient magnitude, our model could be easily altered to allow for changes in zooplankton growth rates with changing ϕ in order to increase quantitative predictive power.

Finally, it is important to note the inherent mismatch between the time scales employed in our model and experiment. The dominant forcing period in natural aquatic ecosystems is one year. In contrast, the SSD approach assumes the limit of infinite period forcing in which species dynamics approach log-linear (as in Fig. 1A) and which maintains analytical tractability (C. A. Klausmeier, *unpublished manuscript*). Numerical results show that this approximation is reasonable for systems forced at the annual scale (C. A. Klausmeier, *unpublished manuscript*). Our laboratory system was forced with an effective period of 16.5–21.5 days; longer periods would have required larger winter dilutions, which would have resulted in less than one rotifer per flask in our 800-mL experimental volumes. Thus, the time scales of our mathematical and laboratory models varied in opposite directions from the natural systems they were intended to mimic, potentially generating discrepancies between our predictions and empirical results. As ϕ decreased in our experiments, the assumptions of the SSD model were better met, which may account for the stronger match between observed and predicted transition times and the better fits seen in supplemental Figs. A1 and A2 (Appendix A).

The growing reality of climate change has necessitated more in-depth examination of the role of seasonal forcing and altered seasonality on the structure and dynamics of natural communities (Walther et al. 2002, Parmesan and Yohe 2003, Menzel et al. 2006, Berger et al. 2007, Cleland et al. 2007, Huber et al. 2008). As increases in average mean temperatures may increase the number of ice-free days temperate lakes experience, the effective length of the growing season is also predicted to increase. How such alterations impact the timing of spring algal blooms and zooplankton population peaks is a vital question facing aquatic ecologists. Our model provides a simple but tractable framework for exploring the dynamic consequences of variation in large-scale seasonal events. We show both theoretically and empirically that the probability of zooplankton population persistence increases with increasing growing period. Furthermore, the timing of zooplankton and algal population blooms depends greatly on the relative length of the growing season with the timing of algal/zooplankton population peaks occurring progressively earlier in the year with increasing growing period. Such advances in the seasonal timing of plankton population peaks have been detected in many long-term data sets (e.g., Winder and Schindler 2004*a*, *b*, Huber et al. 2008). Our model framework could help to better understand the mechanisms underlying such phenological changes. Given the low number of parameters required by the approach, the successional state dynamics framework can be easily altered to address alternative food-web structures while retaining analytical tractability. Moreover, the model's minimal parameter requirement has the advantage of being relatively easy to parameterize empirically and generate quantitative predictions. Thus, compared to more complex, process-based numerical models, the SSD framework could be a more promising approach for generating projections of plankton phenology under future climate warming.

LITERATURE CITED

Berger, S. A., S. Diehl, H. Stibor, G. Trommer, M. Ruhenstroth, A. Wild, A. Weigert, C. Jäger, and M. Striebel. 2007. Water temperature and mixing depth affect timing and intensity of events during spring succession of the plankton. Oecologia 150:643–654.

Cleland, E. E., I. Chuine, A. Menzel, H. A. Mooney, and M. D. Schwartz. 2007. Shifting plant phenology in response to global change. Trends in Ecology and Evolution 22:357–365.

de Senerpont Domis, L. N., W. M. Mooij, S. Hülsmann, E. H. van Nes, and M. Scheffer. 2007. Can overwintering versus diapausing strategy in Daphnia determine match–mismatch events in zooplankton–algae interactions? Oecologia 150: 682–698.

Harris, E. 1989. The *Chlamydomonas* sourcebook: a comprehensive guide to biology and laboratory use. Academic Press, New York, New York, USA.

Hastings, A. 2001. Transient dynamics and persistence of ecological systems. Ecology Letters 4:215–220.

Hastings, A. 2004. Transients: the key to long-term ecological understanding? Trends in Ecology and Evolution 19:39–45.

Haupt, R. L., and S. E. Haupt. 1998. Practical genetic algorithms. Wiley Interscience, New York, New York, USA.

Huber, V., R. Adrian, and D. Gerten. 2008. Phytoplankton response to climate warming modified by trophic state. Limnology and Oceanography 53:1–13.

Ives, A. R., K. Gross, and V. A. A. Jansen. 2000. Periodic mortality events in predator–prey systems. Ecology 81:3330–3340.

Jäger, C. G., S. Diehl, C. Matauschek, C. A. Klausmeier, and H. Stibor. 2008. Transient dynamics of pelagic producer–grazer systems in a gradient of nutrients and mixing depths. Ecology 89:1272–1286.

Kilham, S. S., D. A. Kreeger, S. G. Lynn, C. E. Goulden, and L. Herrera. 1998. COMBO: a defined freshwater culture medium for algae and zooplankton. Hydrobiologia 377:147–159.

Litchman, E., and C. A. Klausmeier. 2001. Competition of phytoplankton under fluctuating light. American Naturalist 157:170–187.

MATLAB. 2006. MATLAB, version 7.2. MATLAB, Natick, Massachusetts, USA.

Menzel, A., et al. 2006. European phenological response to climate change matches the warming pattern. Global Change Biology 12:1969–1976.

Mooij, W. M., et al. 2005. The impact of climate change on lakes in the Netherlands: a review. Aquatic Ecology 39:381–400.

Parmesan, C., and G. Yohe. 2003. A globally coherent fingerprint of climate change impacts across natural systems. Nature 421:37–42.

Scheffer, M., S. Rinaldi, Y. A. Kuznetsov, and E. H. Vannes. 1997. Seasonal dynamics of *Daphnia* and algae explained as a periodically forced predator–prey system. Oikos 80:519–532.

Sommer, U. 1989. Plankton ecology: succession in plankton communities. Springer-Verlag, New York, New York, USA.

Sommer, U., Z. M. Gliwicz, W. Lampert, and A. Duncan. 1986. The PEG-model of seasonal succession of planktonic events in fresh waters. Archive für Hydrobiologie 106:433–471.

SPSS. 2000. SYSTAT, version 10. SPSS, Chicago, Illinois, USA.

Straile, D. 2002. North Atlantic Oscillation synchronizes food-web interactions in central European lakes. Proceedings of the Royal Society of London B 269:391–395.

Straile, D., and R. Adrian. 2000. The North Atlantic Oscillation and plankton dynamics in two European lakes—two variations on a general theme. Global Change Biology 6:663–670.

Van Donk, E., M. Lurling, D. O. Hessen, and G. M. Lokhorst. 1997. Altered cell wall morphology in nutrient-deficient phytoplankton and its impact on grazers. Limnology and Oceanography 42:357–364.

Walther, G. R., E. Post, P. Convey, A. Menzel, C. Parmesan, T. J. C. Beebee, J.-M. Fromentin, O. Hoegh-Guldberg, and F. Bairlein. 2002. Ecological responses to recent climate change. Nature 416:389–395.

Winder, M., and D. E. Schindler. 2004a. Climate change uncouples trophic interactions in an aquatic ecosystem. Ecology 85:2100–2106.

Winder, M., and D. E. Schindler. 2004b. Climatic effects on the phenology of lake processes. Global Change Biology 10:1844–1856.

APPENDIX A

Six supplementary figures (*Ecological Archives* E090-222-A1).

APPENDIX B

A description of the genetic algorithm (*Ecological Archives* E090-222-A2).